

Synthesis and Unusual Physical Behavior of a Photorefractive Polymer Containing Tris(bipyridyl)ruthenium(II) Complexes as a Photosensitizer and Exhibiting a Low Glass-Transition Temperature

Qing Wang, Liming Wang, and Luping Yu*

Contribution from the Department of Chemistry and The James Franck Institute, The University of Chicago, 5735 South Ellis Avenue, Chicago, Illinois 60637

Received July 16, 1998

Abstract: This paper reports the synthesis and characterization of a low- T_g photorefractive (PR) polymer which contains ionic ruthenium complexes as the photogenerator of charge carriers. It was expected that a combination of the highly efficient photocharge generation of the Ru complex, the efficient charge transporting of the conjugated backbone, and the orientational enhancement associated with low- T_g materials would lead to further improvement of PR performances. However, it was very interesting to find that the PR performance of this polymer was limited by the local internal field formed in response to the external electric field by the alignment of ion pairs around the photocharge generation sites. The effects of such a local field on photocharge generation and photorefractivity were investigated through the analyses of the dependence of photocurrent, photorefractive gain, diffraction efficiency, electrooptic activity, and birefringence on the applied field. The dynamic behavior of the PR grating formation was also investigated.

Polymeric photorefractive (PR) materials have been the subject of intense research since the first PR polymer system was disclosed.¹ Part of the stimulation for these research efforts is the wide variety of potential applications of these materials in image processing and optical data storage.² These are multifunctional materials which usually contain the following functional moieties: charge generating and transporting agents, charge trapping sites, and second-order nonlinear optical (NLO) chromophores. Their mechanisms of photorefractivity are very different from those of the conventional inorganic crystals and thus render a great challenge to gain deep insight into their mechanistic aspect.^{3,4}

A popular approach to the preparation of PR polymers is to mix all of the necessary functional species into polymer matrices, forming composites.⁵ For example, large photorefractivity has been achieved in a PR composite based on poly(*N*-vinylcarbazole) (PVK) polymers. Some of the characteristic parameters have matched or even exceeded those of their inorganic counterparts, for example, a nearly 100% diffraction efficiency and 200 cm⁻¹ net optical gain have been obtained.⁶ A general observation in the composite PR polymeric materials is that only those systems with low glass transition temperatures (T_g) (below or slightly above room temperature) give rise to large net optical gain. This phenomena is referred to as the

“orientational enhancement effect”,⁷ in which NLO chromophores can be reoriented under the influence of the space charge field at ambient temperature. This effect leads to a spatial modulation of the birefringence coming from both the optical anisotropy of chromophore and electrooptic (EO) effect, which greatly improves the magnitude of the refractive index grating. In fact, for the low- T_g PR materials, the orientational effect makes a greater contribution to the photorefractive gain than does the linear EO effect.⁸

However, our work mainly focuses on the synthesis and characterizations of fully functionalized materials, in which all functional species are covalently attached to a polymer backbone. Compared with composite PR polymers, fully functionalized PR polymers enjoy the advantage of long-term stability and minimized phase separation. Several systems have been successfully explored, such as functionalized polyurethanes,⁹ functionalized conjugated polymers,¹⁰ and polyimides containing porphyrin and NLO chromophore units.¹¹ More recently, we developed a new PR polymer system, i.e., a hybridized PR polymer that contains an ionic tris(bipyridyl)ruthenium complex as the charge-generating species, a conjugated polymer backbone as the charge transporting channel, and an NLO chromophore.^{12,13} The ruthenium complex was introduced to utilize its efficient photoinduced metal-to-ligand charge-transfer (MLCT)

(1) Ducharme, S.; Scott, J. C.; Twieg, R. J.; Moerner, W. E. *Phys. Rev. Lett.* **1991**, *66*, 1846.

(2) (a) Günter, P.; Huignard, J.-P. Ed. *Photorefractive Materials and Their Applications*; Springer-Verlag: Berlin, 1989; Vol. 2. (b) Schlöter, S.; Haarer, D. *Adv. Mater.* **1997**, *9*, 991. (c) Meerholz, K. *Angew. Chem., Int. Ed. Engl.* **1997**, *36*, 945. (d) Poga, C.; Lundquist, P. M.; Lee, V.; Shelby, R. M.; Twieg, R. J.; Burland, D. M. *Appl. Phys. Lett.* **1996**, *69*, 1047.

(3) Moerner, W. E.; Silence, S. M. *Chem. Rev.* **1994**, *94*, 127.

(4) Yu, L. P.; Chan, W. K.; Peng, Z. H.; Gharavi, A. R. *Acc. Chem. Res.* **1996**, *29*, 13.

(5) Zhang, Y.; Burzynski, R.; Ghosal, S.; Casstevens, M. K. *Adv. Mater.* **1996**, *8*, 111.

(6) Meerholz, K.; Volodin, B. L.; Sandalphon; Kippelen, B.; Peyghambarian, N. *Nature* **1994**, *371*, 497.

(7) Moerner, W. E.; Silence, S. M.; Hache, F.; Bjorklund, G. C. *J. Opt. Soc. Am. B* **1994**, *11*, 320.

(8) Moerner, W. E.; Grunnet-Jepsen, A.; Thompson, C. L. *Annu. Rev. Mater. Sci.* **1997**, *27*, 585.

(9) Yu, L. P.; Chan, W. K.; Bao, Z. N.; Cao, S. *Macromolecules* **1993**, *26*, 2216.

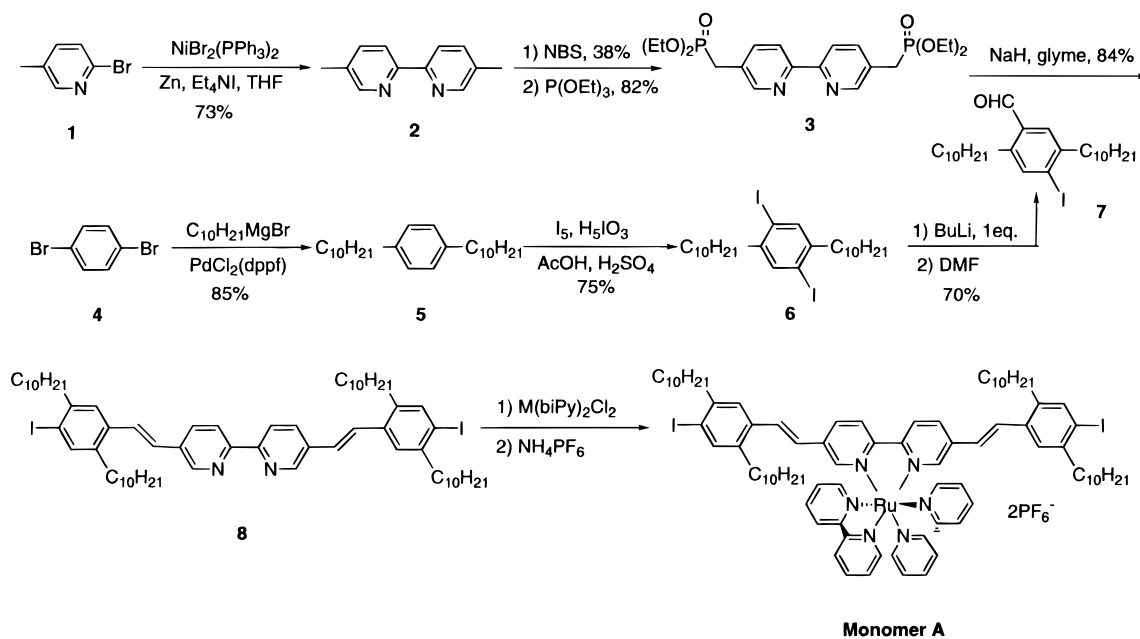
(10) Chan, W. K.; Chen, Y. M.; Peng, Z. H.; Yu, L. P. *J. Am. Chem. Soc.* **1993**, *115*, 11735.

(11) Peng, Z. H.; Bao, Z. N.; Chen, Y. M.; Yu, L. P. *J. Am. Chem. Soc.* **1994**, *116*, 6003.

(12) Peng, Z. H.; Gharavi, A. R.; Yu, L. P. *Appl. Phys. Lett.* **1996**, *69*, 4002.

(13) Peng, Z. H.; Gharavi, A. R.; Yu, L. P. *J. Am. Chem. Soc.* **1997**, *119*, 4622.

Scheme 1. Synthesis of Monomer A



process so that problems of low quantum yield for the photogeneration of charge carriers in organic materials can be addressed. This PR polymer system has displayed greatly enhanced PR performance; a net optical gain of about 200 cm^{-1} was obtained. That is one of the largest net optical gains reported so far. This PR response, however, is mainly due to the linear EO contribution because the polymer exhibits a high glass transition temperature ($130 \text{ }^\circ\text{C}$) and the dipoles of the NLO chromophores cannot be reoriented in responding to the periodical space-charge field. We reasoned that, if the T_g of the polymer was lowered without a large change in the polymer structure, we may have the chance to further enhance the PR performance by combining a highly efficient photocharge generator, an efficient charge transportor, the large EO contribution, and the orientational enhancement associated with low- T_g materials. We succeeded in synthesizing such a polymer containing transition metal complexes and a conjugated system and exhibiting a T_g of $11 \text{ }^\circ\text{C}$. However, detailed physical studies revealed an interesting phenomenon: at high external electric field, the PR efficiency of this polymer was hindered by the local internal field which is induced by ion dipole moment formed between the Ru(II) complex and its counterion (PF_6^-). To our knowledge, this is the first time that such a local field effect on the photocharge generation and the PR response was observed. This kind of local field effect on the photocharge generation efficiency may also be a general issue in other fields. Any electric field assist charge separation processes, such as those in solar cells, xerographic layer, may be subject to such an effect. In this paper, we report the synthesis and physical characterization of a low- T_g conjugated polymer containing Ru(II)-tris(bipyridyl) complexes and pendant NLO chromophores.

Results and Discussion

Synthesis and Structural Characterization. The syntheses of monomers are outlined in the Schemes 1 and 2. 5,5'-Dimethyl-2,2'-bipyridine (**2**) was prepared by homocoupling of 2-bromo-5-picoline (**1**) using a nickel catalyst which was generated in situ by reduction of $\text{NiBr}_2(\text{PPh}_3)_2$ with zinc in the presence of Et_4NI . This approach is advantageous over the method catalyzed by the Raney nickel because its reaction condition is mild and reaction yield is normally better than the

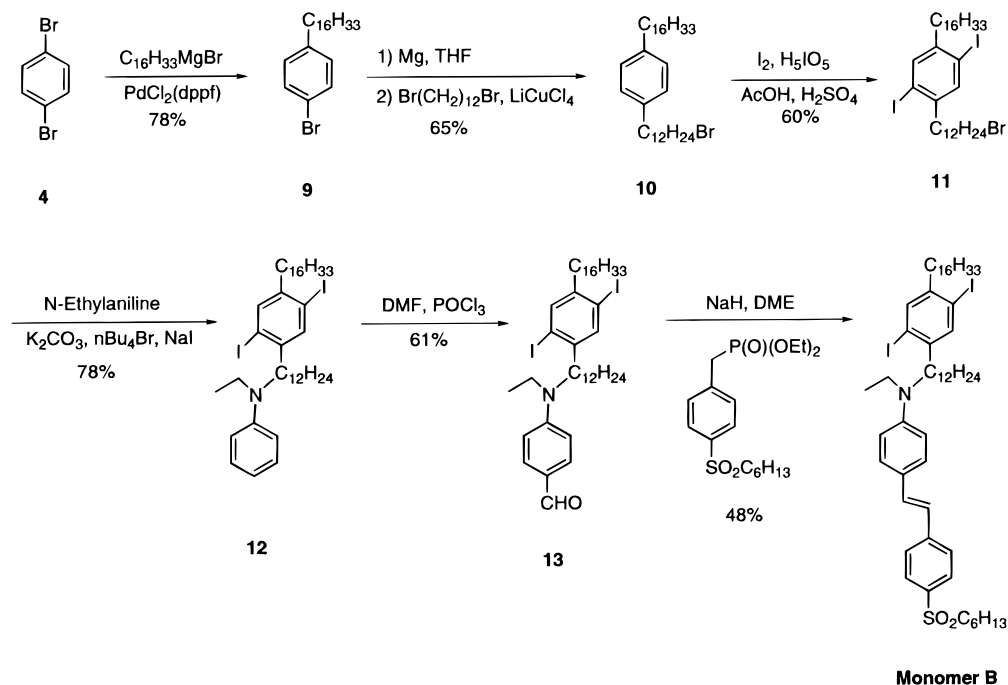
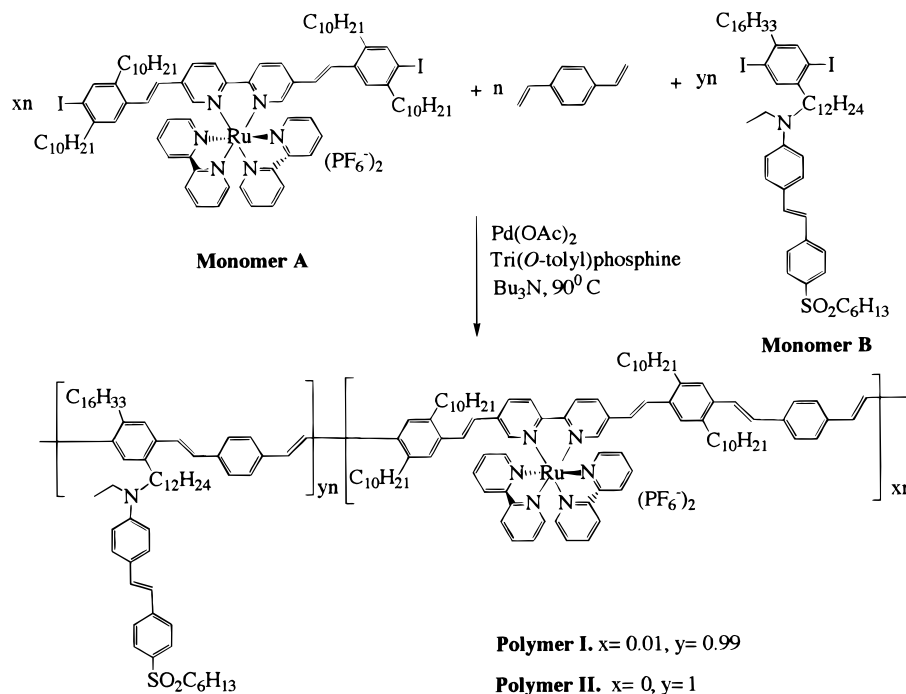
later one.¹⁴ Instead of using alkoxy side chains, long alkyl side chains were introduced into monomers. These side chains help to increase the solubility and processibility of the resulting conjugated polymers and to lower the T_g of polymers. Another advantage of introducing alkyl chain is that the absorption the poly(*p*-phenylenevinylene) (PPV) backbone of the resulting polymer is blue shifted compared to those with alkoxy substituents. This blue-shift minimizes the absorption overlap between the $\pi-\pi^*$ transition of PPV backbone and the MLCT transition of the Ru complex.¹³ Thus, charge carriers can be selectively generated from the Ru complexes center by using a longer wavelength laser (He-Ne, 632.8 nm).

The polymerization was carried out according to Scheme 3, using a catalytic system composed of $\text{Pd}(\text{OAc})_2/\text{P}(o\text{-tolyl})_3/n\text{-Bu}_3\text{N}$ (4%/20%/250%, mole percentage vs monomers). The resulting polymer is soluble in most common organic solvents, such as THF, chloroform, DMF, etc. GPC measurements in THF, using polystyrene as a standard, indicated a number-averaged molecular weight (M_n) of approximately 18 000 with a polydispersity (PD) of ca. 1.9.

The structural characteristics of polymers were provided by ^1H NMR, UV/vis spectroscopy, and elemental analysis. Since the resulting polymers contains only 1% of the Ru complexes, the ^1H NMR spectrum of the polymer is dominated by the chemical shift of the chromophore and the PPV backbone. However, chemical shifts due to the bipyridyl ligand protons (8.0, 8.4 ppm) still can be observed (Figure 1), indicating the incorporation of the ruthenium complex into the polymer. Some small peaks at 5.2 and 5.8 ppm, which are believed to be introduced by side reactions of the Heck reaction,¹⁵ were also found (about 1–2%). Figure 2 shows the UV/vis spectrum of the thin film of the polymer (polymer **I**). The major absorption band around 380 nm is attributed to the absorption of the PPV backbone overlapping with that of the chromophore, which is supported by the similarity of this spectrum with that of the polymer without Ru complexes (polymer **II**) as also shown in Figure 2. For polymer **I**, there is an absorption tail extending

(14) Iyodaa, M.; Otsuka, H.; Sato, K.; Nisato, N.; Oda, M. *Bull. Chem. Soc. Jpn.* **1990**, *63*, 80.

(15) Brenda, M.; Greiner, A.; Heitz, W. *Makromol. Chem.* **1990**, *191*, 1083.

Scheme 2. Synthesis of Monomer B**Scheme 3.** Synthesis of Polymers I and II

beyond 600 nm, which can be assigned to the MLCT absorption of the ruthenium complexes. This extending tail is the most interesting feature because it enables us to photoexcite the polymer mainly through MLCT processes by using a He–Ne laser (i.e., 632.8 nm).

As we expected, the resulting polymer exhibits a relatively low T_g of 11 °C, determined by differential scanning calorimetry (DSC). This low T_g and the good solubility in organic solvents make this polymer easy to be processed into high optical quality films of thickness over 100 nm from its solution.

For the purpose of comparison, a neutral conjugated polymer containing a Cu(II)–porphyrin moiety was synthesized under similar conditions (Scheme 4). The resulting polymer (polymer

III) exhibited an M_n of 18 000 with a PD of 1.88 determined by GPC. The T_g of the polymer was measured by DSC to be 16 °C. The structure of the polymer was studied by elemental analysis, ^1H NMR, and UV/vis absorption spectra. The paramagnetic property of Cu(II) severely broadened the ^1H NMR spectra of the monomer and the polymer. In the UV/vis spectrum (in THF), Q-bands between 500 and 600 nm could be clearly identified. These results indicate that the metalporphyrin moiety was incorporated into the polymer backbone.

Physical Characterization. A. Photorefractive Gain. To study the PR properties of the polymer, the first (also the most important) experiment is the two-beam coupling (2BC) experiment which can determine the PR nature of a material. In this

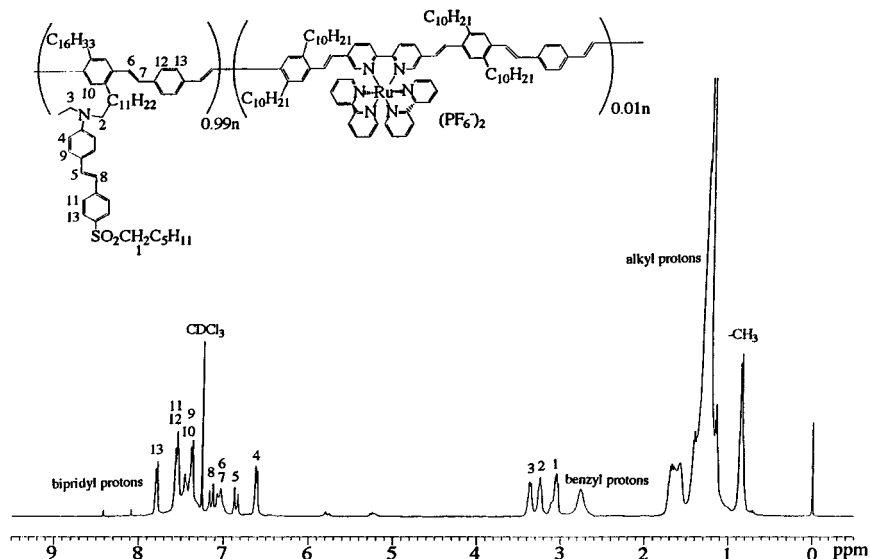
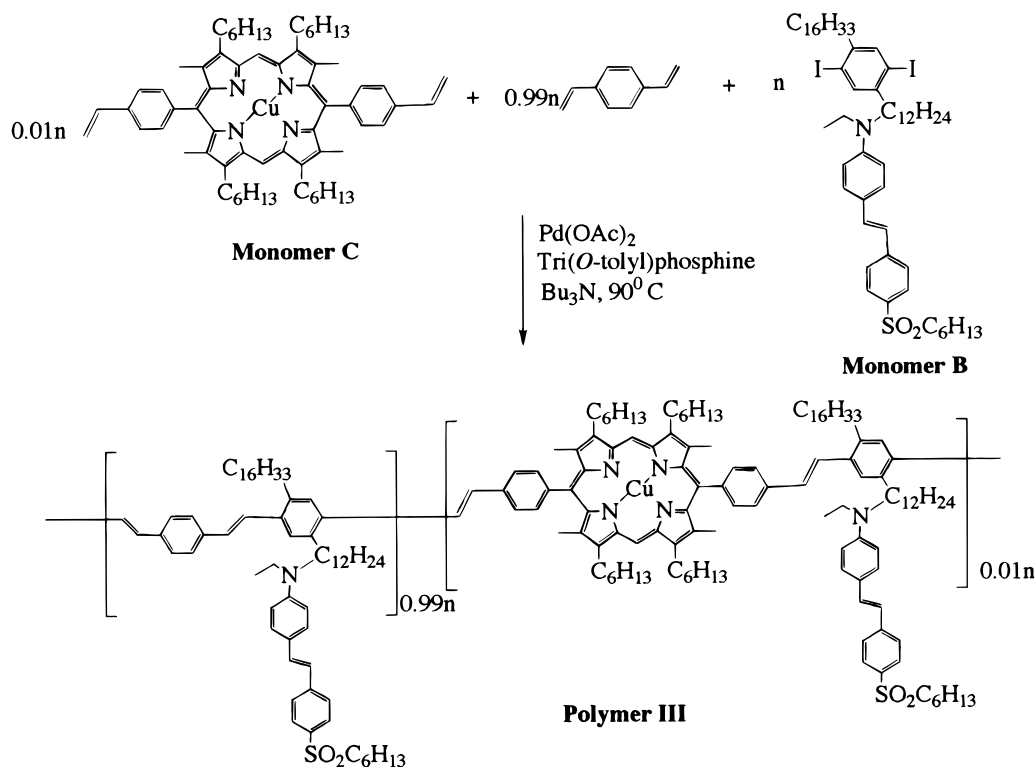


Figure 1. ^1H NMR spectrum of Ru-containing polymer.

Scheme 4. Synthesis of Cu–Porphyrin-Containing Polymer (Polymer III)



experiment, two coherent laser beams intersect inside a PR polymer film and a refractive index grating can be generated. Since the phase of the refractive index grating is shifted in comparison to the illumination pattern, the two writing beams are diffracted into each other's direction by these very gratings, accompanied with asymmetric energy exchange. This feature is cited as the signature of photorefractivity. We performed the 2BC experiment on our polymer film with two *p*-polarized He–Ne laser beams (632.8 nm) of equal intensity ($2 \times 1.6 \text{ W/cm}^2$). The normal of the sample was tilted 52° with respect to the bisector of the writing beams to provide a projection of the grating wave vector along the poling axis. With this geometry, a holographic grating with a spacing of $2.7 \mu\text{m}$ was created in the material (the refractive index of the polymer at 632.8 nm is 1.63). With the applied field on, clear asymmetric energy transfer between the two beams was observed as shown in

Figure 3: one beam gained energy and the other lost energy. As the electric field was turned off, the beam coupling disappeared and the intensities of the both beams returned to their original levels. When the polarity of the applied field was reversed, the gain and loss beams were also switched, as expected, which is due to reversal of the dipole orientation. These experimental results are clear indications that the grating is due to photorefractive effect and not due to thermal or absorption grating.¹⁶ The 2BC gain coefficient (Γ) was calculated according to the following equation:^{2a}

$$\Gamma = \frac{1}{L} \ln \left(\frac{1 + \alpha}{1 - \beta\alpha} \right)$$

(16) Wiederrecht, G. P.; Yoon, B. A.; Wasielewski, M. R. *Science* **1995**, *270*, 1794.

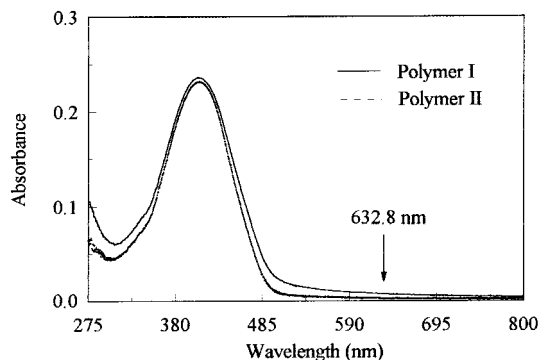


Figure 2. Solid UV/vis spectrum of polymers I and II.

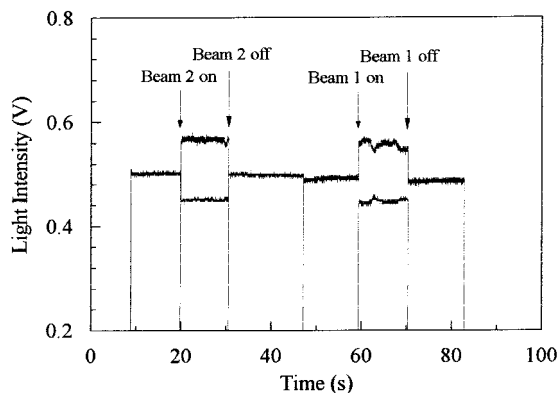


Figure 3. Asymmetric energy transfer at the field of 90 V/μm in the 2BC experiment.

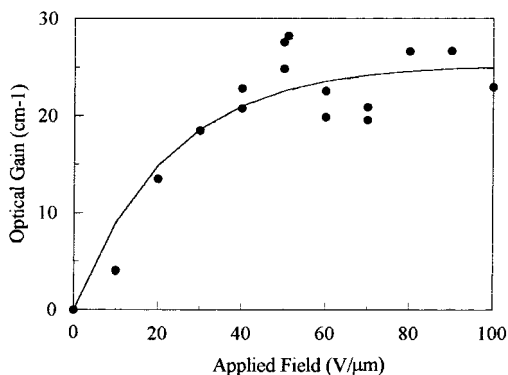


Figure 4. Photorefractive gain coefficient as a function of the applied field.

where α is the ratio of the intensity modulation ($\Delta I_s/I_s$) and β is the intensity ratio of the two incident laser beams (I_s/I_q).

B. Local Field Effect. It is interesting, however, to observe that the optical gain coefficient increases with the external field initially and then levels off when the applied field surpasses about 50 V/μm, as shown in Figure 4. This behavior is quite different from those of the low- T_g composite PR materials, in which the gain coefficient increases nonlinearly with the applied field. Unlike the high- T_g version of this polymer, no net optical gain was observed. At the field of 80 V/μm, an optical gain of 26.6 cm⁻¹ was detected, while the absorption coefficient, α , is 28 cm⁻¹.

To understand this deviation in the behavior of the field dependence of the 2BC gain coefficient, two necessary elements for the PR effect, photoconductivity and field-induced birefringence (which reflects the EO effect of the sample), were investigated. The photocurrent and birefringence as a function of the applied field are shown in Figures 5 and 6. The birefringence exhibits a typical field enhancement behavior

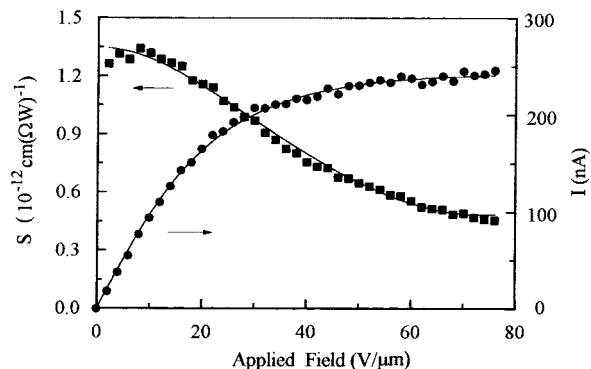


Figure 5. Dependence of photoconductive sensitivity (S) and photocurrent (I) on the applied field.

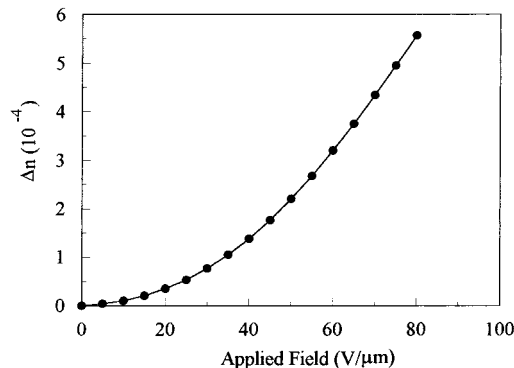


Figure 6. Magnitude of the index modulation versus the applied field.

similar to that of conventional low- T_g composite PR polymers,^{3,5} while the photocurrent shows the same trend in the field dependence as that of the 2BC gain coefficient: at a field of 50 V/μm, the photoconductivity became saturated. It seems that the photoconductive process is the limitation on PR performance.

These results can be attributed to the existence of ionic ruthenium and the low- T_g nature of the material. The counterion pairs of PF₆⁻ and the Ru(II)-tris(bipyridyl) segment form the ionic dipole moment pointing from Ru(II) to (PF₆⁻)₂. The dipole moment is randomly oriented in the absence of an external field. When an external electric field is applied to the PR polymer film, the dipoles of both NLO chromophores and the ionic pairs are readily aligned. The effect of alignment of NLO chromophore dipoles on the local field is uniform throughout the film and is limited due to the thermal randomization. The dipole alignment becomes significant for ionic species in a low- T_g polymer because of the large freedom of local motion of the polymer chains and the high mobility of the ions, PF₆⁻. Meanwhile, the magnitude of the ionic dipole moment also increases with the field due to the increase in the distance between the ion pair and the decrease in the angle between the two subdipoles formed by the ionic Ru complex center with two PF₆⁻ ions which overcomes the repelling force between the two PF₆⁻ ions. This magnitude change of the dipole with the applied field makes the ion-pair field increases superlinearly in response to the external field. As a result, the higher the external field applied, the stronger the counter internal field generated from the ion dipoles, and this counter internal field partially screens Ru(II)-tris(bipyridyl) complex sites from the applied external field.

It is well-known that photogeneration of charge carriers in organic polymers involves a two-step mechanism: the photoexcitation and dissociation of the bound electron-hole pair.¹⁷

(17) Mylinikov, V. In *Advances in Polymer Science*; Springer-Verlag: Berlin Heidelberg, 1994; Vol. 115.

To assist the separation of the bound pairs, an applied field is always needed. Therefore, the photogeneration efficiency of charge carriers is strongly dependent on the local field around the photocharge generation sites. Since the ruthenium complex acts as a photocharge generator, the screen effect due to this ionic dipole field will reduce the photocarrier separation efficiency and cause the photocurrent to saturate. The photoconductive sensitivity (S) could be estimated from the photocurrent (I_{ph}) by the following expression:¹⁸

$$S = \frac{I_{ph}L}{AVI_0}$$

where L is the sample thickness, A is the illumination area, V is the applied voltage, and I_0 is the intensity of illumination of the beam. As a result of the decrease in photogeneration efficiency of charge carriers, the photoconductive sensitivity decreases as the increase of the applied field (Figure 5).

According to the "standard PR theory" developed for inorganic ferroelectric single crystals, the saturation of optical gain can possibly be explained by the decrease of the effective trap density at the high field. But, the decrease in the effective trapping centers should lead to the increase of the photoconductive sensitivity with the external field.¹⁹ This is clearly in contrast with our experimental results that the photoconductive sensitivity decreased dramatically with the increase of the external field (Figure 5). The most reasonable explanation must be that the dipole field induced by ion pairs limits charge generation rate and further the steady-state space-charge field. Unfortunately, the "standard PR theory" does not predict the relationship of the space-charge field with the charge generation rate.²⁰ This theory was obtained under many simplified assumptions, especially under the condition that no thermal and electric-induced detrapping occurs after the trapping of the carrier. In reality, for organic PR materials, especially for those low- T_g materials, the trapped charge could be more easily detrapped than that in inorganic PR materials because of the amorphous nature. If the detrapping rate is large enough, the condition of space-charge fields being limited by trap density could never be reached and the space-charge field would be a function of photoconductivity.²¹ The PR optical gain therefore became saturated at high field.

This screen effect was also reflected in degenerate four-wave mixing (DFWM) experiments. In this experiment, the two s-polarized beams (632.8 nm, 2×1.45 W/cm²) were used as writing beams and the grating formed in the material was read out with a weak p-polarized reading beam (632.8 nm, 230 mW/cm²) counter-propagating to one of the writing beams. The diffraction efficiency, η , defined as the ratio of the diffracted to incident reading beam power, was recorded. Because the diffraction efficiency is determined by the amplitude of the index grating, a behavior similar to the optical gain is expected if the index grating is formed mainly due to the photorefractive effect. As shown in Figure 9, the value of η increased with the applied field and became saturated at 0.5% at the field of 50 V/ μ m. When the pump beam was blocked, the diffracted signal dropped immediately.

The spacing of the space-charge field in the 2BC experiment is about 2.7 μ m, which is more than 3 orders of magnitude larger

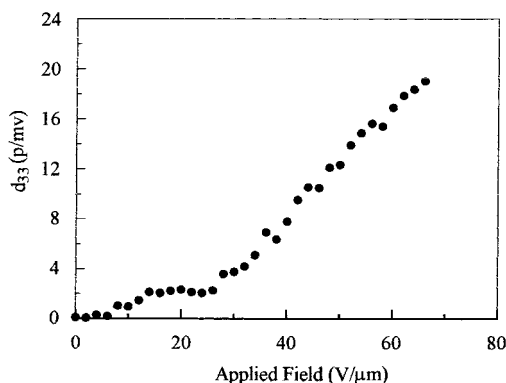


Figure 7. Second-harmonic coefficient, d_{33} , value as a function of the applied field.

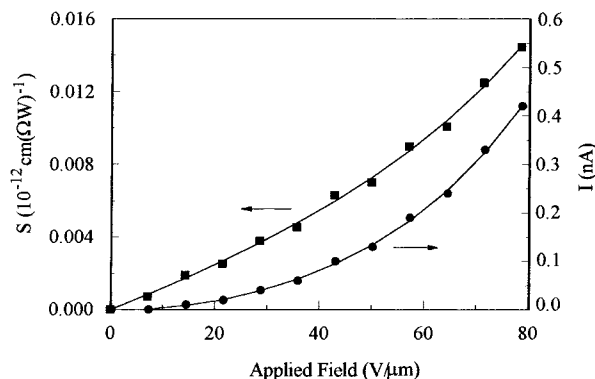


Figure 8. Field dependence of photoconductive sensitivity (S) and photocurrent (I) of Cu-porphyrin-containing polymer.

than the diameter of the polymer backbone. Therefore, this internal field induced by ionic dipole moment is a local effect compared to the variation of the space-charge field. Because the Ru(II)-tris(bipyridyl) complex is only 1 mol % in the polymer system, large amounts of the segments with the NLO chromophore are not influenced by this local internal field. Therefore, the birefringence due to the alignment of the dipole moments of the NLO chromophores and Pockel effect should not exhibit any saturation. This is indeed the case as shown in Figure 6. Second-harmonic generation (SHG) experiments indicate a field-dependent behavior of the SHG signal similar to that of most of the NLO polymers. The NLO chromophores could be effectively aligned at room temperature by applying an external field, and the effect of the ionic dipole field was not observed (Figure 7).

To confirm experimentally that such a local field effect is significant in the ionic metal-containing polymer, another novel low- T_g polymer containing a neutral copper porphyrin as the photocharge generator has been synthesized (Scheme 4). This polymer exhibits an absorption coefficient of 23 cm⁻¹ at 632.8 nm. The field dependence of the photocurrent and photoconductive sensitivity are shown in Figure 8. In contrast to the behavior of the ionic ruthenium containing polymer, this Cu-porphyrin polymer displays field enhancement behavior in both photocurrent and photoconductive sensitivity. It is worth pointing out that the absolute value of the photoconductive sensitivity of the Cu-porphyrin polymer is about 2 orders of magnitude smaller than that of polymer containing Ru(II) complexes. This may be attributed to the less efficient MLCT process in the Cu-porphyrin polymer and the fast relaxation of the excited states caused by the unpaired spin in Cu(I) center.

Although the internal field induced by the ion dipole limits the PR performance in our low- T_g materials, this limitation

(18) Schildkraut, J. S. *Appl. Phys. Lett.* **1991**, *58*, 340.

(19) Pfister, G.; Mort, J.; Grammatica, S. *Phys. Rev. Lett.* **1976**, *37*, 1360.

(20) (a) Valley, G. C.; Klein, M. B. *Opt. Eng.* **1983**, *22*, 704. (b) Schildkraut, J. S.; Cui, Y. *J. Appl. Phys.* **1992**, *72*, 5055.

(21) Moharam, M. G.; Gaylord, T. K.; Magnusson, R.; Young, L. J. *Appl. Phys.* **1979**, *50*, 5642.

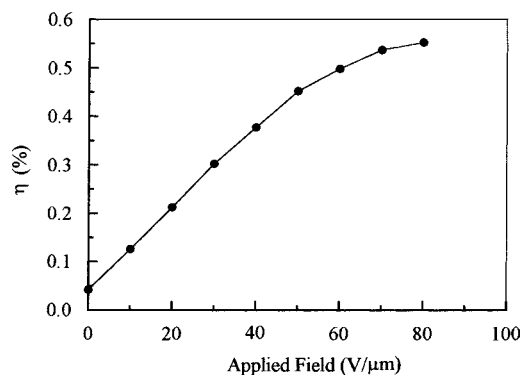


Figure 9. Dependence of the diffraction efficiency on the applied field.

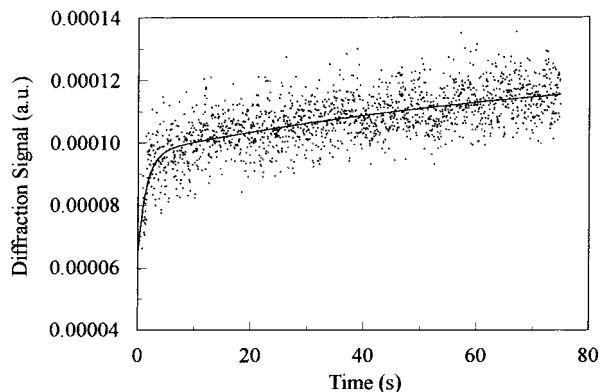


Figure 10. Time dependence of the diffraction signal ($E = 30 \text{ V}/\mu\text{m}$) probed by DFWM.

should not present in high- T_g materials since the local motion of the polymer chain is so small that the ion dipole cannot be effectively aligned by the applied field at room temperature. In fact, the photocarrier separation and mobility at zero external field could be further enhanced by the internal field produced by the aligned ion pairs and the dipoles of NLO chromophores in PR polymer films after corona poling at an elevated temperature. It seems to us that the enhancement of photoconductivity and the stability of the aligned NLO chromophore are responsible for the extraordinarily large PR optical gain at zero field in our previously reported PR polymer that contains an ionic Ru(II)-tris(bipyridyl) complex and possesses a T_g as high as 130°C .¹³

C. Dynamics of Grating Formation. The dynamics of the holographic grating formation were studied by measuring the time constants of the grating formation and their electric field dependence in the DFWM experiment. A typical behavior of grating formation is illustrated in Figure 10, in which the writing beams are turned on at time $t = 0$. A fast initial rise in the diffraction signal is observed, and then slows down after approximately 5 s of writing time. The rapid initial rise accounts for about 80% of the saturated value of diffraction efficiency. Quantitative information about the grating growth can be obtained by an empirical two-exponential fit of the following form to the data of diffraction intensity:

$$\eta(t) \sim \{E_{\text{scf}}[1 - \exp(-t/\tau_f)] + E_{\text{scs}}[1 - \exp(-t/\tau_s)]\}^2$$

where E_{scf} , E_{scs} , τ_f , and τ_s are the four fitting parameters. The fast component of the diffraction efficiency is indicated by the first term of the equation, while the slow component is represented by the second term of the equation. Figure 11 shows the dependence of the initial grating growth rate and the slow rate on the applied field. High electric field markedly increases

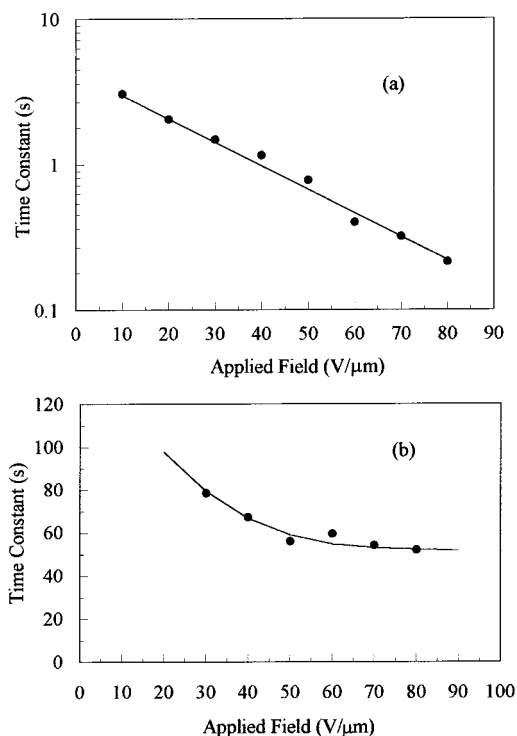


Figure 11. Electric field dependence of the fast component of the time constants of the grating formation (a) and the slow component of the time constants of the grating formation (b).

the speed of the initial grating formation (Figure 11a). At a field of $80 \text{ V}/\mu\text{m}$, the initial grating writing time constant is around 0.21 s, which is comparable with that of the fastest known PR polymers. Such a fast response time may be attributed to large charge carrier mobility and facile NLO chromophore alignment in this type of material. It was known that there are many different channels that contribute to photoconductivity and photorefractive charge storage.²² Since the charge-transporting processes in organic amorphous materials are usually very dispersed, the formation of space-charge field does not bear an exponential relationship to the photoconductivity. In our polymer, although the screening from the ion pairs limited the photocharge generation efficiency, the transporting of charge carriers is not affected since the ion-pair field is still a local effect compared to the drift length, which is typically in the order of submicrons. The mobility of the charge carriers—the hopping process—can still be greatly enhanced by the applied field. Therefore, the initial space-charge field could be formed through certain fast carrier transporting channels without the limitation by the carrier generation rate. The behavior of the slow rate is interesting and reflects the effect of the ionic dipole field on the photogeneration rate of the charge carriers (Figure 11b). The formation speed slows down because of the limitation on the photocharge generation and makes the slow component almost independent of the applied field at a high external field (Figure 11b).

Conclusions

A novel low- T_g PR polymer which contains tris(bipyridyl)-ruthenium(II) as a photosensitizer has been synthesized. Its PR properties have been studied through the analyses of the dependence of photoconductivity, optical gain coefficient, birefringence, EO activities, and diffraction efficiency on the

(22) Jone, B. E.; Ducharme, S.; Liphard, M.; Goodnesseker, A.; Takacs, J. M.; Zhang, L.; Athalye, R. *J. Opt. Soc. Am. B* **1994**, *11*, 1064.

field. It was found that the ionic dipole moments in this low- T_g ionic PR polymer are easily aligned and generate an internal field to screen the photocharge generation site from the external applied field. Such a screen effect limits the photocharge generation efficiency and PR performance at a high applied field. Saturation was observed in the field dependence of photoconductivity, PR optical gain coefficient, and diffraction efficiency. We believe that this investigation of the local field effect on photocharge generation should be useful enlightenment for development and optimization of new PR polymers. The above results indicate that to synthesize high-performance PR polymers, a low- T_g PR polymer containing neutral Ru complexes should be explored to fully utilize the efficient MLCT process and orientational enhancement.

Experimental Section

Tetrahydrofuran (THF) and ethyl ether were purified by distillation over sodium chips and benzophenone. The *p*-divinylbenzene was separated from a mixture of *p*-divinylbenzene and *m*-divinylbenzene according to the literature procedure.²³ All of the other chemicals were purchased from Aldrich Chemical Co. and used as received unless otherwise noted. Compound **3** and monomer **C** were prepared according to refs 13 and 24.

Synthesis of Monomers: Compound 2. To the nickel catalyst prepared from $\text{NiBr}_2(\text{PPh}_3)_2$ (14.38 g, 19.35 mmol), zinc (6.33 g, 96.83 mmol), and Et_4Ni (16.60 g, 64.55 mmol) in THF (90 mL) was added a solution of 11.1 g (64.5 mmol) of 2-bromo-5-picoline (**1**) in THF (40 mL). After being stirred at 50 °C for 20 h, the mixture was poured into 2 M aqueous ammonia (500 mL), followed by addition benzene (250 mL) and ethyl acetate (250 mL). A brown cloudy solution was given. After filtration, the filtrate was extracted with benzene/AcOEt (1:1). The organic layer was washed with water, dried over anhydrous MgSO_4 , and evaporated in vacuo. The residue was separated by flash chromatography (silica gel, benzene/AcOEt (10:1)) to give 5,5'-dimethyl-2,2'-bipyridine (**2**) (4.3 g, 73%). $^1\text{H NMR}$ (CDCl_3 , ppm): δ 2.35 (s, 6H, $-\text{CH}_3$), 7.61 (d, $J = 8.08$ Hz, 2H, aromatic protons), 8.24 (d, $J = 8.09$ Hz, 2H, aromatic protons), 8.49 (s, 2H, aromatic protons).

Compound 5. 1-Bromodecane (22.92 g, 0.1035 mol) in 18 mL of ether was added to a suspension containing Mg (2.5 g, 0.1028 mol) and ether (25 mL) at a rate to maintain the refluxing of the reaction mixture. After the addition was complete, the mixture was further heated to reflux for half an hour. The solution was then added dropwise into a mixture containing 1,4-dibromobenzene (**4**) (11.0 g, 0.0466 mol), $\text{PdCl}_2(\text{dppf})$ (0.76 g, 0.93 mmol), and 40 mL of ether. The resulting mixture was refluxed overnight and then poured into water. After removal of the catalyst residue (red precipitate) by filtration, the filtrate was extracted with ether. The combined organic layer was then washed with water and dried by MgSO_4 . Evaporation of the solvent gave a brown oil which was distilled under vacuum, yielding a slight yellow oil (14.19 g, 85%, bp 213–214 °C at 0.2 mmHg). $^1\text{H NMR}$ (CDCl_3 , ppm): δ 0.87 (t, $J = 6.58$ Hz, 6H, $-\text{CH}_3$), 1.25–1.29 (m, 32H, alkyl protons), 1.57 (m, 4H, alkyl protons), 2.55 (t, $J = 7.81$ Hz, 4H, benzyl protons), 7.07 (s, 4H, aromatic protons).

Compound 6. A mixture of compound **5** (11.48 g, 0.032 mol), iodine (10.17 g, 0.04 mol), H_5IO_6 (3.8 g, 0.017 mol), acetic acid (30 mL), 30% sulfuric acid (15 mL), and chloroform (15 mL) was stirred at 80 °C for 48 h and then poured into water. The crude product was collected by filtration and washed with water and cold ethanol. Recrystallization from ethanol/ethyl acetate (6:1) gave a colorless solid (14.66 g, 75%). $^1\text{H NMR}$ (CDCl_3 , ppm) δ 0.88 (t, $J = 6.58$ Hz, 6H, $-\text{CH}_3$), 1.27–1.35 (m, 28H, alkyl protons), 1.52–1.57 (m, 4H, alkyl protons), 2.59 (t, $J = 7.81$ Hz, 4H, benzyl protons), 7.59 (s, 2H, aromatic protons).

Compound 7. *n*-BuLi (3.8 mL, 2.5 M solution in hexane, 9.424 mmol) in 15 mL of ether was added dropwise in the 35 mL of an ether solution of compound **6** (5.75 g, 9.425 mmol) at 0 °C. After the addition of BuLi was completed, DMF (1.09 mL, 14.13 mmol) in 5 mL of ether

was added dropwise into the solution. The resulting mixture was stirred at room temperature for 2 h and poured into water. The organic layer was collected, and the aqueous layer was extracted with ether. The combined organic layer was washed with water and dried over MgSO_4 . After removal of the solvent, the crude product was chromatographed (silica gel, hexane/ethyl acetate (20:1)) to give a colorless solid (3.37 g, 70%). $^1\text{H NMR}$ (CDCl_3 , ppm): δ 0.88 (t, $J = 6.59$ Hz, 6H, $-\text{CH}_3$), 1.26–1.35 (m, 28H, alkyl protons), 1.58 (m, 4H, alkyl protons), 2.71 (t, $J = 8.03$ Hz, 2H, benzyl protons), 2.88 (t, $J = 7.99$ Hz, 2H, benzyl protons), 7.59 (s, 1H, aromatic protons ortho to CHO), 7.75 (s, 1H, aromatic protons meta to CHO), 10.21 (s, 1H, $-\text{CHO}$).

Compound 8. Sodium hydride (0.37 g, 15.42 mmol) was added to a solution of compound **7** (5.27 g, 10.29 mmol) in 25 mL of 1,2-dimethoxyethane (DME). The resulting suspension was stirred for 10 min at room temperature. Compound **3** (2.35 g, 5.15 mmol) in DME (10 mL) was then added dropwise. The mixture was refluxed overnight. After the solution was cooled to room temperature, water and dichloromethane were added. The crude product was precipitated out and separated by filtration. Recrystallization from dichloromethane gave a bright yellow solid (5.07 g, 84%). $^1\text{H NMR}$ (CDCl_3 , ppm): δ 0.85–0.89 (m, 12H, $-\text{CH}_3$), 1.25–1.55 (m, 56H, alkyl protons), 1.69 (m, 8H, alkyl protons), 2.64–2.72 (m, 8H, benzyl protons), 7.05 (d, $J = 16.14$ Hz, 2H, vinyl protons), 7.39 (d, $J = 16.12$ Hz, 2H, vinyl protons), 7.44 (s, 2H, aromatic protons meta to I), 7.64 (s, 2H, aromatic protons ortho to I), 7.98 (d, $J = 8.38$ Hz, 2H, 4-pyridine protons), 8.43 (d, $J = 8.30$ Hz, 2H, 3-pyridine protons), 8.79 (s, 2H, 6-pyridine protons). Anal. Calcd for $\text{C}_{66}\text{H}_{98}\text{N}_2\text{I}_2$: C, 67.60; H, 8.36; N, 2.39. Found: C, 67.41; H, 8.30; N, 2.40.

Monomer A. A solution of compound **8** (0.306 g, 0.261 mmol), *cis*-dichlorobis(2,2'-bipyridine)ruthenium(II) hydrate (0.126 g, 0.261 mmol), and 25 mL of methoxyethanol was stirred at 140 °C for 4 h. After being cooled to room temperature, the solution was added into an $(\text{NH}_4)\text{PF}_6$ (0.425 g, 2.61 mmol) aqueous solution. The solid precipitated out and was purified by chromatography (silica gel, dichloromethane/methanol (20:1)) (0.274 g, 56%). $^1\text{H NMR}$ (CDCl_3 , ppm): δ 0.85 (t, $J = 6.54$ Hz, 12H, $-\text{CH}_3$), 1.18–1.48 (m, 64H, aliphatic protons), 2.53–2.64 (m, 8H, benzyl protons), 6.79 (d, $J = 16.42$ Hz, 2H, vinyl protons), 7.30 (d, $J = 16.42$ Hz, 2H, vinyl protons), 7.42 (s, 2H, aromatic protons meta to iodo), 7.46 (m, 4H, aromatic protons), 7.56 (s, 2H, aromatic protons ortho to iodo), 7.63 (s, 2H, aromatic protons), 7.76 (dd, $J = 5.10$ Hz, 4H, aromatic protons), 7.95 (d, $J = 8.37$ Hz, 4H, aromatic protons), 8.38 (d, $J = 8.79$ Hz, 2H, aromatic protons), 8.41 (m, 6H, aromatic protons). Anal. Calcd for $\text{C}_{86}\text{H}_{114}\text{N}_6\text{I}_2\text{P}_2\text{F}_2\text{Ru}$: C, 55.04; H, 6.07; N, 4.48; I, 13.52. Found: C, 55.06; H, 6.09; N, 4.47; I, 13.60.

Compound 9 was obtained from 1,4-dibromobenzene (**4**) in 78% yield, following a procedure similar to that described for compound **5**. $^1\text{H NMR}$ (CDCl_3 , ppm): δ 0.88 (t, $J = 6.70$ Hz, 3H, $-\text{CH}_3$), 1.28 (m, 26H, alkyl protons), 1.57 (m, 2H, alkyl protons), 2.55 (t, $J = 7.60$ Hz, 2H, benzyl protons), 7.05 (d, $J = 8.30$ Hz, 2H, aromatic protons), 7.38 (d, $J = 8.30$ Hz, 2H, aromatic protons).

Compound 10. Compound **9** (7.18 g, 18.8 mmol) in 20 mL of THF was added dropwise into a mixture of Mg (0.55 g, 22.2 mmol), 10 mL of THF, and a small crystal of iodine at such a rate that the reaction mixture maintained self-refluxing. After the addition was complete, the mixture was heated to reflux for half an hour. The resulting Grignard reagent was transferred by a needle to a mixture containing 1,12-dibromododecane (9.25 g, 28.18 mmol), Li_2CuCl_4 (2.8 mL of 0.1 M THF solution, 28.18 mmol), and 20 mL of THF. The resulting mixture was stirred overnight at room temperature and then poured into water. The mixture was extracted with dichloromethane. The combined organic layer was washed successively with saturated aqueous NaHCO_3 solution and water and dried over MgSO_4 . The solvent was removed by rotary evaporation, and the residue was recrystallized from acetone to give a colorless solid of compound **10** (6.71 g, 65%). $^1\text{H NMR}$ (CDCl_3 , ppm): δ 0.87 (t, $J = 6.59$ Hz, 3H, $-\text{CH}_3$), 1.25–1.29 (m, 40H, alkyl protons), 1.38 (m, 2H, alkyl protons), 1.55 (m, 4H, alkyl protons), 1.85 (m, 2H, alkyl protons), 2.58 (t, $J = 7.65$ Hz, 4H, benzyl protons), 3.41 (t, $J = 6.88$ Hz, 2H, $-\text{CH}_2\text{Br}$), 7.08 (s, 4H, aromatic protons).

Compound 11 was obtained from compound **10** in 60% yield, following a procedure similar to that described for compound **6**. ^1H

(23) Strey, B. T. *J. Polym. Sci., Part A* **1965**, *3*, 265.

(24) Bao, Z.; Chen, Y.; Yu, L. P. *Macromolecules* **1994**, *27*, 4629.

NMR (CDCl₃, ppm): δ 0.87 (t, J = 6.60 Hz, 3H, -CH₃), 1.26–1.32 (m, 40H, alkyl protons), 1.39 (m, 2H, alkyl protons), 1.55 (m, 4H, alkyl protons), 1.85 (m, 2H, alkyl protons), 2.59 (t, J = 7.82 Hz, 4H, benzyl protons), 3.41 (t, J = 6.85 Hz, 2H, -CH₂Br), 7.59 (s, 2H, aromatic protons).

Compound 12. A mixture of compound **11** (4.13 g, 5.15 mmol), *N*-ethylaniline (1.30 mL, 10.31 mmol), potassium carbonate (2.14 g, 15.48 mmol), tetrabutylammonium bromide (0.166 g, 0.515 mmol), and sodium iodine (7 mg, 0.047 mmol) in toluene (12 mL) was refluxed overnight. The mixture was then poured into water and extracted with dichloromethane. The organic layer was separated and washed with water and dried over MgSO₄. After the solvent was evaporated, the residue was purified by flash chromatography (silica gel, hexane/dichloromethane (2:1)) (3.37 g, 78%). ¹H NMR (CDCl₃, ppm): δ 0.88 (t, J = 6.58 Hz, 3H, -CH₃), 1.14 (t, J = 7.04 Hz, 3H, -NCH₂CH₃), 1.22–1.31 (m, 42H, alkyl protons), 1.54 (m, 6H, alkyl protons), 2.58 (t, J = 7.83 Hz, 4H, benzyl protons), 3.24 (t, J = 7.63 Hz, -CH₂N-), 3.34 (quintet, J = 7.04 Hz, 2H, -NCH₂CH₃), 6.64 (m, 3H, aromatic protons), 7.20 (t, J = 7.24 Hz, 2H, aromatic protons), 7.59 (s, 1H, aromatic protons).

Compound 13. To a ice-cooled DMF (2 mL, 25.83 mmol) was added phosphorus oxychloride (0.762 g, 4.96 mmol) dropwise. The solution was stirred at 0 °C for 1 h and at room temperature for another 1 h. Compound **12** (3.8 g, 4.517 mmol) in 7 mL of DMF was then added dropwise to the mixture, and the resulting solution was stirred at 90 °C overnight. The solution was poured into water and extracted with dichloromethane. The separated organic layer was washed with water and dried. After the solvent was evaporated, the residue was chromatographed (silica gel, hexane/ethyl ether (2:1)) to give a colorless liquid (2.40 g, 61%). ¹H NMR (CDCl₃, ppm): δ 0.88 (t, J = 6.53 Hz, 3H, -CH₃), 1.18–1.33 (m, 45H, alkyl protons), 1.61 (m, 6H, alkyl protons), 2.58 (t, J = 7.73 Hz, 4H, benzyl protons), 3.25 (t, J = 7.60 Hz, -CH₂N-), 3.32 (quintet, J = 7.01 Hz, 2H, -NCH₂CH₃), 6.67 (d, J = 8.44 Hz, 2H, aromatic protons), 7.59 (s, 1H, aromatic proton), 7.72 (d, J = 8.44 Hz, 2H, aromatic protons), 9.69 (s, 1H, -CHO).

Monomer B. Sodium hydride (0.145 g, 6.04 mmol) was added to a solution of compound **13** (2.91 g, 3.348 mmol) in 10 mL of DME. The suspension was stirred for 10 min at room temperature, followed by dropwise addition of the solution of diethyl 4-(hexyl sulfone)benzyl phosphate (1.26 g, 3.348 mmol) in 5 mL of DME. The resulting solution was stirred at 80 °C overnight and then poured into water. The mixture was extracted with dichloromethane. The combined organic layer was washed with water and dried. After removal of the solvent, the residue was separated by chromatography (silica gel, hexane/ethyl ether (4:1)) to give a greenish yellow solid (1.756 g, 48%). ¹H NMR (CDCl₃, ppm): δ 0.87 (m, 6H, -CH₃), 1.17–1.69 (b, 59H, alkyl protons), 2.58 (t, J = 7.63 Hz, 4H, benzyl protons), 3.07 (t, J = 8.14 Hz, 2H, -SO₂-CH₂-), 3.23 (t, J = 7.31 Hz, 2H, -CH₂N-), 3.35 (quintet, J = 6.85 Hz, 2H, -NCH₂CH₃), 6.64 (d, J = 8.82 Hz, 2H, aromatic protons), 6.85 (d, J = 16.20 Hz, 1H, vinyl proton), 7.12 (d, J = 16.15 Hz, 1H, vinyl proton), 7.40 (d, J = 8.73 Hz, 2H, aromatic protons), 7.59 (m, 4H, aromatic protons), 7.80 (d, J = 8.40 Hz, 2H, aromatic protons). Anal. Calcd for C₅₆H₈₇SNI₂O₂: C, 61.58; H, 7.96; N, 1.28. Found: C, 61.65; H, 7.98; N, 1.23.

Polymerization. A typical polymerization procedure follows: Tri-*n*-butylamine (0.32 mL, 1.34 mmol) was added to the mixture of monomer **A** (0.010 g, 0.00540 mmol), monomer **B** (0.5890 g, 0.5400 mmol), *p*-divinylbenzene (0.070 g, 0.545 mmol), palladium acetate (4.9 mg, 0.0217 mmol), and tri-*o*-tolylphosphine (32.9 mg, 0.108 mmol) in 5 mL of DMF. The reaction mixture was stirred at 90 °C overnight under a nitrogen atmosphere and then poured into methanol. The precipitate was collected, redissolved in chloroform, and filtered to

remove the catalyst residue. The filtrate was concentrated and precipitated into methanol, followed again by filtration and reprecipitation. The resulting polymer was further purified by extraction in a Soxhlet extractor with methanol for 24 h and then was dried under a vacuum at 40 °C for 24 h.

Polymer I. Anal. Calcd for C_{66.3}H_{95.27}N_{1.05}O_{1.98}S_{0.99}P_{0.02}F_{0.12}Ru_{0.01}: C, 81.79; H, 9.78; N, 1.51; Ru, 0.10. Found: C, 81.07; H, 9.87; N, 1.41; Ru, 0.08.

Polymer II. Anal. Calcd for C₆₆H₉₅NO₂S₁: C, 82.08; H, 9.84; N, 1.45. Found: C, 81.90; H, 9.92; N, 1.31.

Polymer III. Anal. Calcd for C_{66.54}H_{15.68}N_{1.04}O₂SCu_{0.01}: C, 82.04; H, 9.82; N, 1.49. Found: C, 81.41; H, 9.57; N, 1.44.

Characterization. The ¹H NMR spectra were collected on a Bruker 500-MHz FT NMR spectrometer. A Shimadzu UV-2401PC UV/vis was used to record the UV/vis spectra. Thermal analyses were performed by using the DSC-10 system from TA Instruments with a heating rate of 10 °C/min under a nitrogen atmosphere. Elemental analyses were performed by Atlantic Microlab, Inc., except for the ruthenium analyses, which were done by Galbraith Laboratories, Inc. Molecular weights were measured with a Water RI GPC system using polystyrene as the standard and THF as the eluent.

The films for PR characterization were made by sandwiching polymers between two indium–tin oxide (ITO) covered glass substrates. The thickness of the film was fixed around 104 nm with the help of polyimide spacers.

The photoconductivity measurements were performed on about 26 mm thick film sandwiched between Au and ITO electrodes at a wavelength of 632.8 nm using a photocurrent method.²⁵ The photocurrent was measured by monitoring the voltage drop on a resistor which is in series with the film capacitor.

Second-order NLO properties of polymeric films were characterized by a second-harmonic generation experiment. A mode-lock Nd:YAG laser (Continuum-PY 61 C-10, 10-Hz repetition rate) was used as the light source. The second harmonic of the fundamental wave (1064 nm) generated by the polymer sample was detected by a photomultiplier (PMT) and then amplified and averaged in a boxcar integrator. The d_{33} value was obtained by assuming $d_{33} = 3d_{31}$ with a quartz crystal as the reference sample.

The electric field induced birefringence was measured using an ellipsometric method with a crossed-polarizer geometry on the same sample as in PR measurements.²⁶ The sample normal was tilted at 45° with respect to the incident light. The polarization of the incident light was 45° with respect to the incident plane.

Two-beam coupling experiments were performed using a He–Ne laser (632.8 nm, 30 mW) as the light source. The laser beam (*p*-polarized) was split into two beams with equal intensity (2×1.6 W/cm²), which were intersected in the polymer film at 24.5°. The transmitted intensities of the two beams were monitored by two calibrated diode detectors, and the data were recorded by a computer.

Acknowledgment. This work was supported by the National Science Foundation and Air Force of Scientific Research. Support from the National Science Foundation Young Investigator program is gratefully acknowledged. This work also benefited from the support of the NSF MERSEC program at the University of Chicago.

JA9825130

(25) Li, L.; Lee, J. Y.; Yang, Y.; Kumar, J.; Tripathy, S. K. *Appl. Phys. B* **1991**, *53*, 279.

(26) Grunnet-Jepsen, A.; Thompson, C. L.; Twieg, R. J.; Monermer, W. E. *J. Opt. Soc. Am. B* **1998**, *15*, 901.